2016

Laser Micromachining of Contactless RF Antenna Modules for Payment and Cards and Wearable Objects

Matthias John
Trinity College Dublin, matthias.john@tudublin.ie

Recommended Citation

Matthias, J., Conneely, A.J. & Ammann, M.J. (2016). Laser Micromachining of Contactless RF Antenna Modules for Payment Cards and Wearable Objects. *International Congress on Applications of Lasers & Electro-Optics (ICALEO)*San Diego, CA, USA, 16th October 2016.

LASER MICROMACHINING OF CONTACTLESS RF ANTENNA MODULES FOR PAYMENT CARDS AND WEARABLE OBJECTS

Paper M501

Alan J. Conneely[1], Gerard M. O'Connor[1], Matthias John[2], Max J. Ammann[3], Darren Molloy[4], Mustafa Lotya[4], David Finn[4]

[1] National Centre for Laser Applications, NUI Galway, Galway, Ireland
[2] CONNECT, Trinity College Dublin, Ireland
[3] Antenna & High Frequency Research Centre, Dublin Institute of Technology, Dublin, Ireland
[4] Amatech Group Ltd., Spiddal, Ireland

Abstract

The use of contactless payment methods for consumer transactions is becoming increasingly popular - 1.1 billion contactless transactions were made by Visa cardholders across Europe in the 12 months to July 2015 (€12.6 billion total value). Typically the contactless payment process uses a Radio Frequency (RF) enabled smartcard or a Near Field Communication (NFC) enabled smartphone. In order to ensure continued market acceptance and repeat usage the contactless operation must be robust, quick and efficient. This paper describes the development of an inductively coupled contactless smartcard utilising UV DPSS laser micromachining to fabricate the novel antenna structures from copper laminated epoxy tape. The design of the antenna modules was supported by device modelling using electromagnetic simulation software. Iterative laser ablated antenna prototypes were tested using a Vector Network Analyser to determine the optimum resonant frequency in the 13.56 MHz RFID range and a commercial automated RF test station to measure contactless functionality to EMVCO and ISO14443 standards. An antenna design toolkit was developed based on parameters such as kerf width, number of antenna loops, track width, pitch, antenna DC resistance, etc.

The translation of the laser ablated antenna designs from smartcards to wearable objects, such as wristbands, is also presented.

Introduction

Metallic money was first used in 700 BC and it has been the main form of payment for all types of transactions[1] since then and the demise of cash and its replacement by other payment forms has been predicted numerous times over the years. However in recent years the use of payment cards for consumer transactions has significantly overtaken the use of cash as shown in figure 1.

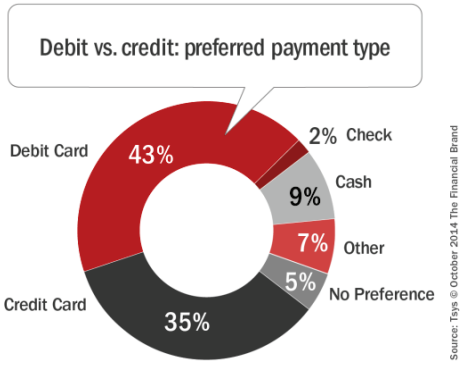

Figure 1: Breakdown of preferred payment methods in the US. Source: TSYS 2014 Consumer Payments Study

Figure 2: Left: Example of contactless payment transaction. Right: Logo for contactless capability.

The technology of payment cards has evolved greatly since the introduction of the first credit card in 1951. Until relatively recently the primary technology was the magnetic stripe but this is being superseded by

'chip & pin', which utilises an encrypted integrated circuit (IC) on each card with a PIN provided by the user as authentication, and contactless 'Tap and Go' for lower value transactions. The interaction from the point of sale (POS) terminal to the payment card IC is either via the physical contact pad or contactless using Radio Frequency (RF) communication, see figure 2. The main format for payment cards is the Dual Interface Card (DIC) which enables both contacted and contactless functionality, see figure 3 for a schematic of dual interface card. The number of dual interface cards in use is predicted to grow significantly over the coming years, see figure 4, as the popularity of contactless use increases.

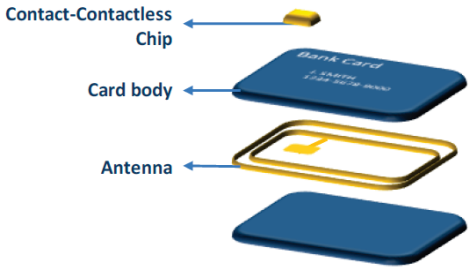

Figure 3: Schematic of internal construction of dual interface card with physical interconnection to chip. Source: Frost & Sullivan[5].

Although the dual interface format provides many advantages for the consumer it provides increased challenges for the card provider as the cost of manufacture and ownership is significantly higher than the contact only card. The increased cost is brought about by:

- requirement for RF antenna circuitry within the card body
- increased complexity of production
- reduced robustness and reliability leading to shorter lifetimes

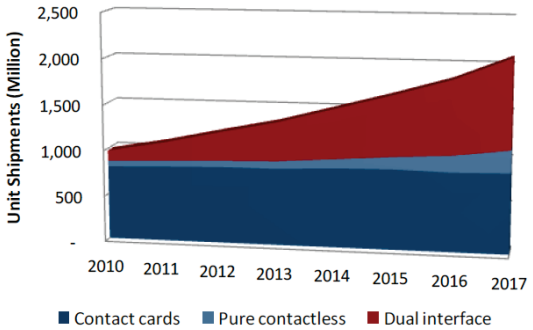

Figure 4: Predicted growth in global shipments of dual interface cards. Source: Frost & Sullivan[5]

The physical interconnection between the RF antenna in the card body and IC module is the primary source of increased production cost and reliability issues. A typical lifetime of 2-3 years is a requirement for payment cards which can be a challenge. Therefore a key innovation in the industry has been the development of secondary RF coupling between the card IC and the card booster antenna, see figures 5, 6, and 7, which eliminates the need for the physical interconnection[2,8,9].

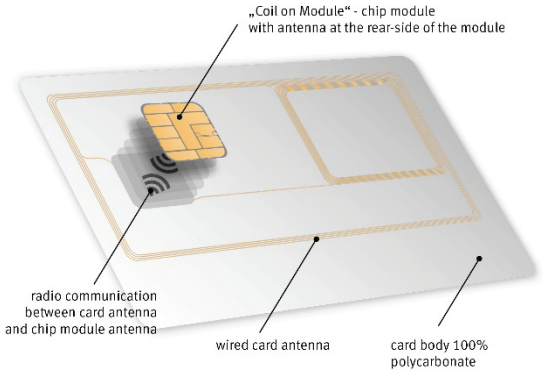

Figure 5: Schematic of 'Coil on Module' technology to remotely connect IC to card inlay 'booster' antenna. Source: Infineon.

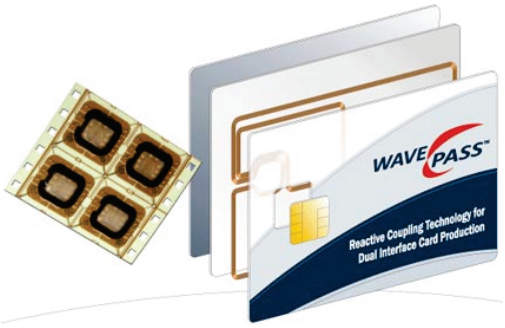

Figure 6: Reactive Coupling module and card antenna card that eliminates the need for physical interconnection. Source: Amatech Group[9]

Contactless card operating standards

The communication between the contactless card and reader terminal is based on a carrier radio frequency (RF) of 13.56 MHz as used in RFID technology. In this case the card is a passive device and the card works by harvesting power via inductive coupling from the reader signal. The load modulated RF sub-carriers generated by the card transponder IC are used to transfer the data between card and reader, see figure 7. The communication baud rate determines the frequency of the sub-carriers relative to the carrier

signal. The furthest distance a card is able to harvest enough power to communicate its UID (Unique Identification number is the serial number given to RFID chips when manufactured) to a polling reader, is defined as the activation range. The reader continuously transmits requests for a UID query. As a card gets within close enough proximity of the reader it is able to harvest power from the magnetic field to power up and respond to the query.

The operation of contactless payment cards are governed by the ISO 14443:2016 and the EMVCo standards[2,6,7] and some of the key requirements are outlined in table 1.

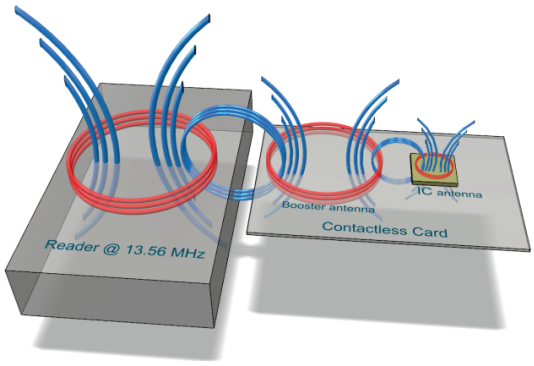

Figure 7: Inductive coupling of reader and card transponder using secondary IC antenna module for power harvesting and communication

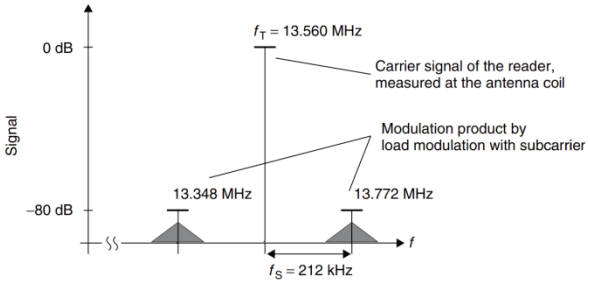

Figure 8: Example of load modulated sidebands and sub-carriers of the RF signal

Table 1: Key specifications for Dual Interface Cards

Standards	1. ISO14443 2. EMVCo 3. ISO/IEC 7813
Activation Range (cm)	4
ID-1 Size (mm)	85.6 x 53.98
Card thickness (µm)	800
Module thickness (µm)	500
Contact Pad Size (mm)	6 pin: 10.6 x 8.0 8 pin: 12.6 x 11.4

Typically lithographic based chemical etching is used for large scale production of the module antennas for smart cards. However the use of laser ablation methods in microelectronic applications, such as for copper PCB machining, is a significant and growing market[3,4].

This paper describes the use of laser micromachining techniques to produce innovative designs and increased performance for the IC module antennas for use in inductively coupled contactless cards and wearable objects.

Experimental details

Materials

This development project used industry standard printed circuit board (PCB) materials sourced from Isola. Table 2 details the PCB properties which is based on an FR4 glass-reinforced epoxy laminate substrate coated with either single-sided Copper or double-sided Copper, see figure 9.

Table 2: PCB material properties

PCB Copper Sheet (Ounce)	Copper Thickness (µm)	Sheet Resistance (mΩ)	FR4 Substrate thickness (µm)
½	17	1	100
1	34	0.5	100

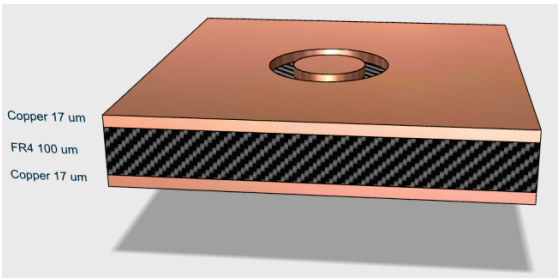

Figure 9: Schematic of double sided copper PCB material

Laser System Configuration

The laser source used for the copper ablation was a frequency tripled 355 nm DPSS Q-switched laser source (Coherent AVIA-X). The laser was coupled with a galvanometer scanner (Scanlab Hurryscan 10)

and f-theta lens (100 mm effective focal length) for beam motion, see figure 10 and table 3. The calculated spot size for the standard laser configuration is 16 µm with a working field of ~60 x 60 mm. The galvo scanner motion was controlled by the LaserDesk software (Scanlab).

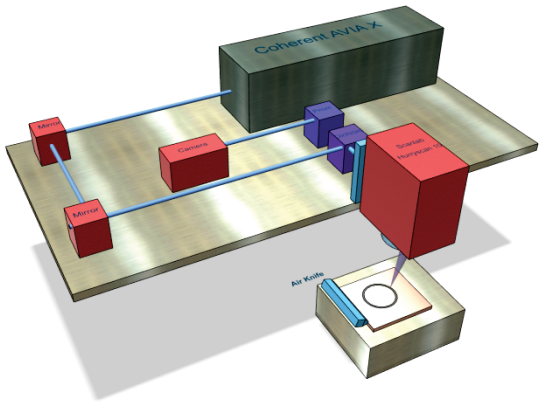

Figure 10: Schematic of laser system at NCLA used for machining of antenna designs

In terms of fixturing, a custom vacuum hold down stage was used to maintain the flatness of the copper PCB material. A 75 mm long air-knife (Meech) operating at 3 bar at the work surface ensured that machining fume and debris was rapidly removed from the work-zone.

Table 3: Laser system configuration used for antenna ablation

Laser Source	Coherent AVIA X
Wavelength (nm)	355
Pulse Width (ns)	<30 (up to 60kHz)
M^2	1.2
Beam Diameter (mm)	3.5
Galvo Scanner	Scanlab Hurryscan 10
f-theta lens effective focal length (mm)	100 (Telecentric)
Spot size (µm)	16
Software	Scanlab LaserDesk

RF Test Samples

Functioning antenna modules were fabricated by soldering the appropriate transponder integrated circuit (IC) chip (NXP, Infineon) to the laser ablated antenna structure, see figure 14. The RF performance of the antenna was measured by mounting the module on a standard Transponder antenna test card (deciphe-it) or integrating to the complete dual interface card with inbuilt booster module, see figure 11.

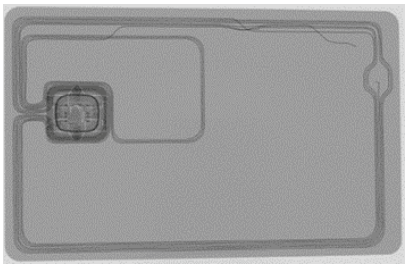

Figure 11: 2D X-Ray Radiograph of dual interface payment card (Amatech Wavepass) showing internal booster and module antenna

RF Test Equipment

The following RF characterisation tools were setup and utilised as part of the study:

- Vector Network Analyser (VNA)
  - Array Solutions VNA 2180DS
  - Primary tool used to measure the RF performance (impedance and frequency response), for a particular module design
  - A key aspect of the module performance is to accurately tune the resonant frequency to the desired 13.56 MHz of the card reader.

- Polling Reader
  - Deciphe-it RFID reader is an ISO 14444A and ISO 14443B compatible proximity RFID read/write device operating at 13.56 MHz.
  - The reader is able to inspect, test, and personalise transponders and is fully compatible with the requirements of the ICAO (International Civil Aviation Organization).
    The reader is used to test basic functionality of a contactless card by polling the card and returning the UID of the RFID chip in the card. When the reader antenna is mounted on a precision height gauge, it is used to measure the activation range of a contactless card.

- Microprocess

- MicroPross Contactless Test Station Premium with MicroBot, see figure 12.
- The Microprossis used for automated measurement system of the data transfer performance for the module
- The system is used to measure compatibility with the industry standard specifications

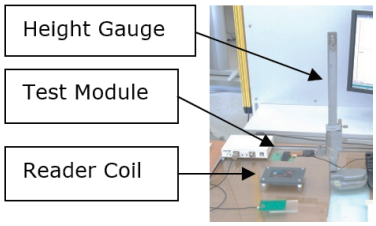

Figure 12: Top - VNA and Polling reader used to measure resonant frequency, activation/read range. Bottom – Microprossystem to measure performance compatibility with industry standards.

RF Modelling and Simulation

Modelling and simulation of the antenna designs was used to support and complement the results from the laser generated prototypes. Finite element electromagnetic simulation software with a frequency domain solver was used to model and analyse various antenna configurations. Simulation CAD models were derived from designs for various module sizes, pitch and track widths as well as metallisation thickness.

The transponder module is a resonant LC circuit. The resonant frequency, f_0, is dependent on the inductance and capacitance in the circuit and is given by

$$f_0 = 1/(2\pi\sqrt{LC})$$

The inductance, L, is proportional to the number of turns in the coil and inversely proportional to the track width. The capacitance, C, is dependent on the gap between the tracks (pitch) and the chip capacitance.

Chip impedance was modelled using a lumped element capacitor to tune the antenna. Figure 13 shows a simulation model of a booster antenna with a 6 contact pad transponder.

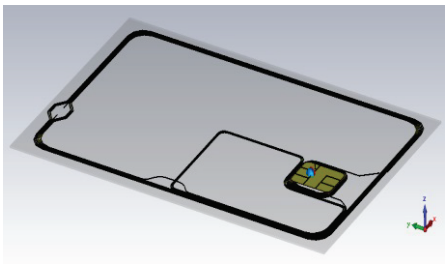

Figure 13: Simulation model of booster antenna and transponder

Designs were analysed and optimised in terms of inductance and resistance of the coupling coil (number of turns), resonance frequency, electromagnetic field strengths generated by the antennas. Figure 14 shows the coil inductance and resistance for various coil geometries and metallisation thicknesses. These results indicate that the metallization thickness has little impact on the inductance of the coil which is primarily determined by the number of antenna turns. A small drop in resistance was observed for thicker metallization. There is a strong dependence on the size of the module (6 or 8 contact pad) with higher inductance and resistance in the larger modules. These simulation results informed antenna and material design decisions and enabled the development of a design toolkit.

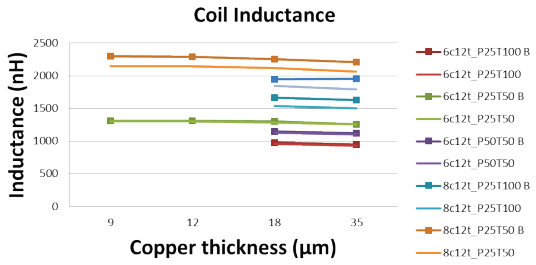

(a)

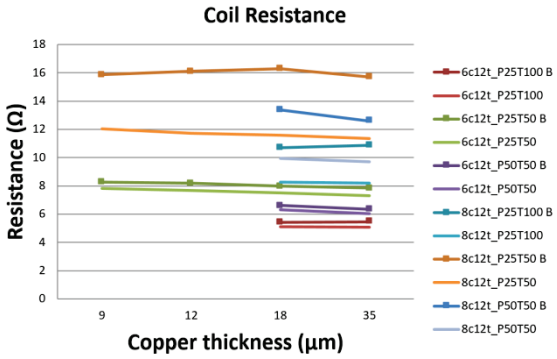

(b)

Figure 14: Simulated coil inductance (a) and resistance (b) versus metallisation thickness for various coupling coil geometries.

Experimental Results

Laser Process Development

A series of laser process development trials were conducted to determine the optimal parameters in terms of quality and throughput. The following factors were key process:

- Complete electrical isolation with minimal debris within ablated kerf
- Narrow kerf to enable increased machining resolution for antenna design
- Minimal heat affected zone (HAZ) to avoid damage to electrical track
- Minimal damage to FR4 substrate to ensure long-term robustness of antenna structure. Excessive epoxy damage can lead to delamination of the copper layer.

Studies identified that a kerf widths in the range of 15 µm to 25 µm provided the optimal combination of isolation, resolution and throughput for the 17 µm copper thickness, see figure 15. This resolution of the laser machining is a key advantage compared to other production methods such as chemical etching which is limited to ~75 µm separation. This means that a greater number of coil turns can be fabricated per given area, see figure 16. A number of different parameter combinations can be found to match the various process requirements and a sample set is provided in table 4.

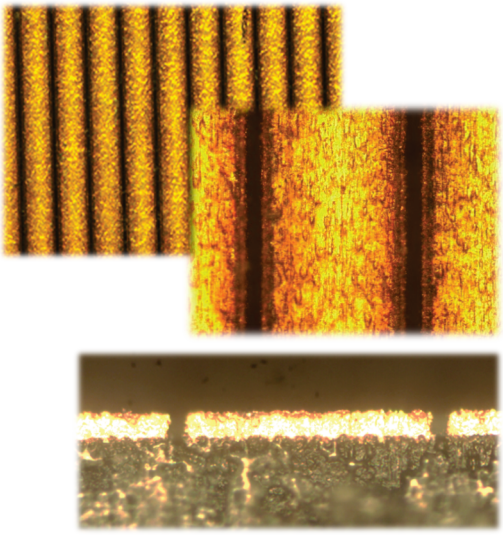

Figure 15: Top - Example of laser machined tracks (~16 µm kerf, 190 µm wide track) in 17 µm double-sided copper tape. Bottom – Cross-section of ablated tracks with minimal heat affected zone in FR4 epoxy substrate

Table 4: Sample process parameter set used for copper (17 µm) antenna processing

Average Power (W)	4.5
Repetition Rate (kHz)	90
Pulse Energy (µJ)	50
Scan Speed (mm/s)	400
Number of Passes	4
Antenna Tool Path Length (mm)	625
Cycle Time (s)	6.5

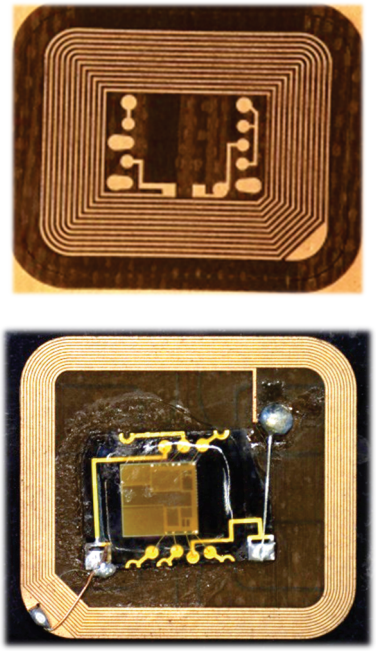

Figure 16: Top – Example of chemical etched antenna. Bottom – laser ablated antenna module with soldered transponder IC.

Tuning of antenna design

The resonant frequency of the antenna is governed by the interaction of the antenna design and transponder IC electrical characteristics (capacitance, inductance, etc). For a given transponder IC, the resonant frequency of the module is tuned via the design of the antenna. An antenna design toolkit can be developed

based on the impact of the various design factors including:

- Conductor type and thickness
- Number of antenna loops
- Active antenna area
- Track width
- Track pitch
- Antenna conductor length

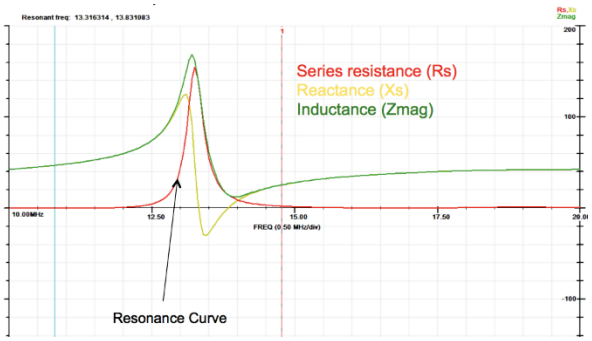

Figure 17: Typical curve from VNA for analysis of antenna performance (Resonance Frequency of 13.3 MHz is shown)

The VNA produces an equivalent serial resistance (Rs) versus frequency graph, see figure 17. In this configuration the resonant frequency is defined as the freqency where the peak Rs value is maximum. This Rs, or resonance curve, gives an approximate indication of the bandwidth and Q (quality factor) of the system, i.e. a wider curve with lower amplitude indicates a higher bandwidth. The Resonance Curve should be wide enough to cover the desired side lobes (as in figure 8) to allow optimum data transfer between card and reader.

The available space for the module antenna is constrained by the module size specification, see table 1. Therefore the track pitch (distance between antenna tracks/loops) and track width (width of copper track) have a direct relationship on the other factors such as number of antenna loops and active antenna area. By producing samples where specific variables are held constant the impact of these variables can be determined. This knowledge is then used to enable an antenna design to be tuned to the resonant frequency in order to achieve optimal performance.

As shown in figure 17, increasing the track width, while keeping number of loops and track pitch constant, tends to increase the resonant frequency. While in figure 18, increasing the track pitch, while keeping number of loops and track width constant, also tends to increase the resonant frequency.

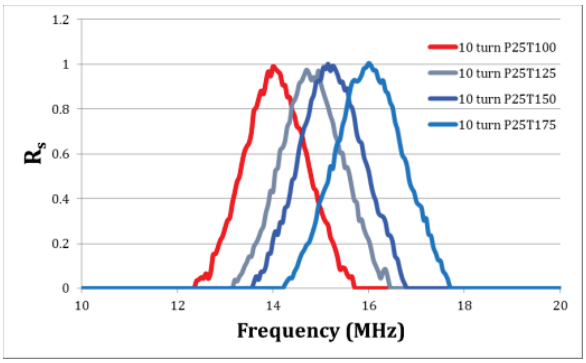

Figure 17: VNA results showing the influence of track width (100 µm to 175 µm) on resonant frequency.

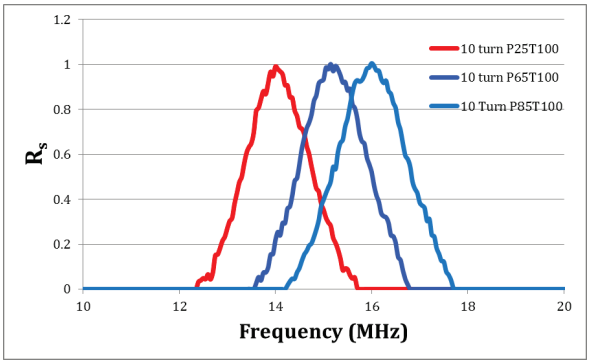

Figure 18: VNA results showing influence of track pitch (25 µm to 85 µm) on resonant frequency.

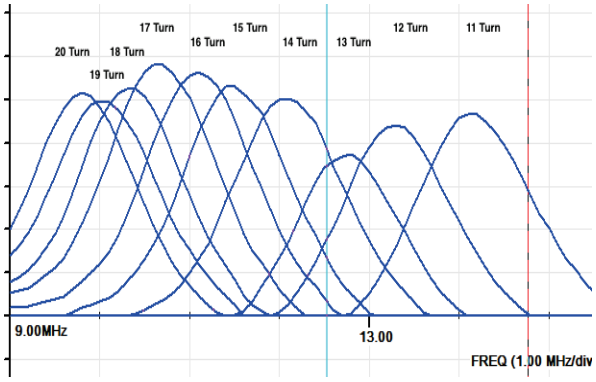

Figure 18: Impact of antenna design (number of antenna loops) on Resonant Frequency.

As shown in figure 18, increasing the number of turns reduces the resonant frequency of the module. Table 5 shows how the tuning of the module antenna affects activation distance.

Table 5: Activation Range for various antenna designs

Antenna	Resonant Frequency (MHz)	Actvation Range (mm)
11 Turn	14.2	42
12 Turn	13.4	43
13 Turn	12.7	41
14 Turn	12.1	40
15 Turn	11.5	38
16 Turn	11.1	37
17 Turn	10.7	35
18 Turn	10.4	35
19 Turn	10.1	34
20 Turn	9.8	32

Wearable Payment Objects

The antenna designs and production methods used for the dual interface payment card can also be utilised for the rapidly growing wearable market. While new industry standards are under development for this new market an activation distance of 4 cm from the reader remains the target in order to allow ease of use. As the wearable payment object operates in pure contactless mode only the metal contact pad is no longer required. In effect the removal of the metal contact pad which acts as shielding can make it easier to achieve the activation distance target. Innovative antenna designs and integration methods[9] have enabled the wearable objects to meet the existing EMV industry standards, see figure 19, 20.

Figure 19: Wearable payment object in a wristband design using a laser ablated antenna module.

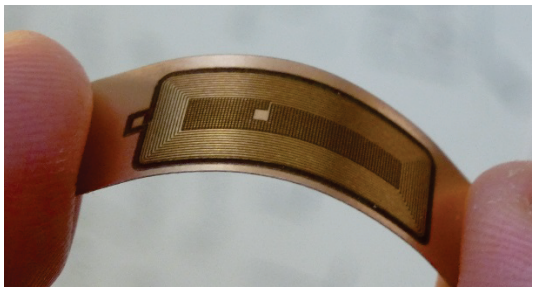

Figure 20: Elongated flexible antenna module for wristband payment object.

Conclusion

The following conclusions can be made from this study:

- UV nanosecond laser ablative machining is very effective for the production of RF antennas in copper PCB materials
- Robust electrical isolation can be achieved while incurring minimal substrate damage
- The achieveable resolution of a 20 µm kerf in 17 µm copper is better than that of chemical etching (~75 µm)
- The reconfigurability of laser machining means that antenna design iterations can be fabricated and functionally tested within a day
- Results of functional testing can be fed into the design process to enable tuning of the antenna geometry
- It has been shown that computer simulation can also be used to predict the RF performance of the modules which enables design decisions
- Antenna module designs and laser fabrication methods have been translated to create functioning wearable payment objects.

Acknowledgements

This work was supported under the Enterprise Ireland Innovation Partnership programme (Project: IP/2013/0265).

This work was conducted under the framework of the Inspire programme, funded by the Irish Government's Programme for Research in Third Level Institutions, Cycle 4, National Development Plan 2007-2013.

References

Book

[1] Evans, D. S.; Schmalensee, R. (2009). Innovation and Evolution of the Payments Industry. In R. E. Litan and M. N. Baily, Moving Money: The Future of Consumer Payments (pp. 36-76). Washington DC: Brookings Press.

[2] Finkenzeller, K. (2010) RFID Handbook Fundamentals and applications in contactless smart cards, radio frequency identification and near-field communication, Third Edition. Wiley ISBN: 978-0-470-69506-7

Journal

[3] Tunna, L., Kearns, A., O'Neill, W., Sutcliffe, C. J., (2001) Micromachining of copper using Nd:YAG laser radiation at 1064, 532 and 355 nm wavelengths, Optics Laser Technol., 33, pp. 135–143

[4] Alwaidh, A., Sharp, M., French, P., (2014) Laser processing of rigid and flexible PCBs, Optics and Lasers in Engineering, Volume 58, July 2014, Pages 109-113, ISSN 0143-8166,

Report

[5] White Paper: Are you looking for the world-class dual interface solution? Frost & Sullivan, 2011

Standard

[6] EMV Contactless Specifications for Payment Systems 2015, EMVCo

[7] ISO/IEC 14443:2016 Identification cards -- Contactless integrated circuit cards -- Proximity cards

Patent

[8] Finn, D., Lotya, M. (2016, Granted) Laser ablating structures for antenna modules for dual interface smartcards. US 9272370 B2

[9] Finn, D., Lotya, M., Molloy, D., (2014, Application) Smartcard with coupling frame and method of increasing activation distance of a transponder chip module. US 2014/0361086 A1

Meet the Authors

Alan Conneely is the Centre Manager of the National Centre for Laser Applications (NCLA) in NUI Galway, Ireland. He received an MSc in laser materials processing from NUI Galway and has over 20 years experience in laser materials processing research with a particular focus on micro-machining applications utilising short and ultra-short pulse lasers.